BICM-ID Using Extended Mapping and Repetition Code with Irregular Node Degree Allocation

Dan Zhao
Japan Advanced Institute of Science and Technology (JAIST), Japan
Email: dan.zhao@jaist.ac.jp

Axel Dauch
Information Technology
University of Ulm, Germany
Email: Axel.Dauch@gmx.de

Tad Matsumoto
Japan Advanced Institute of Science and Technology (JAIST), Japan
Email: matumoto@jaist.ac.jp
and
Center for Wireless Communication at University of Oulu, Finland
Email: tadashi.matsumoto@ee.oulu.fi

Abstract—**Performances of BICM-ID systems strongly depend on the matching between mapping rule and code structure. This paper proposes a combined use of extended mapping (EM) and simple repetition code. Even with such a simple structure, turbo cliff happens at a value range of signal-to-noise power ratio (SNR) 1~2dB to the Shannon limit. This paper then introduces check node as well as irregular node degree allocation to the proposed structure described above, so that we can flexibly change the shape of the decoder EXIT curve. It is shown that EXIT analysis and chain simulation results exactly match each other.**

Keywords - extended mapping; repetition code; irregular node allocation; EXIT analysis; turbo cliff

I. INTRODUCTION

Bit-Interleaved Coded Modulation with Iterative Detection/Decoding (BICM-ID) [1] has been recognized as being a bandwidth efficient coded modulation and transmission scheme, of which transmitter is comprised of a concatenation of encoder and bit-to-symbol mapper separated by a bit interleaver. Iterative detection-and-decoding takes place at the receiver, where extrinsic log likelihood ratio (LLR) obtained as the result of the maximum *a* posteriori probability (MAP) algorithm for demapping/decoding is forwarded to the decoder/demapper via de-interleaver/interleaver, and used as the *a* priori LLR for decoding/demapping, according to the standard turbo principle.

Performances of BICM-ID have to be evaluated by the convergence and asymptotic properties [2], which are represented by the threshold signal-to-noise power ratio (SNR) and bit error rate (BER) floor, respectively. In principle, since BICM-ID is a serially concatenated system, analyzing its performances can rely on the area property [3] of the extrinsic information transfer (EXIT) chart. Therefore, the transmission link design based on BICM-ID falls into the issue of matching between the demapper and decoder EXIT curves. Various efforts have been made in the seek of better matching between the two curves for minimizing the gap while still keeping the tunnel open, aiming, without requiring heavy detection/decoding complexity, at achieving lower threshold SNR and BER floor. Reference [4] introduces a technique that makes good matching between the detector and decoder EXIT curves using low density parity check (LDPC) code in multiple input multiple output (MIMO) spatial multiplexing systems.

It has been believed that a combination of Gray mapping and Turbo or LDPC codes achieves the best performance comparing with other combinations for BICM-ID. However, Ref. [5] proposes another approach towards achieving good matching between the two curves by introducing different mapping rules, such as anti-Gray mapping, which allows the use of even simpler codes, such as convolutional codes, and with which still it is possible to achieve BER pinch-off (corresponding to the threshold SNR). Another good idea that can provide us with design flexibility is extended mapping (EM) presented by [6], [7], [8] where with 2^m-QAM, more than m bits, l_{map}, are allocated to one signal point in the constellation. With this mapping rule, the left-most point of the demapper EXIT function has a lower value than with the Gray mapping, but the right-most point becomes higher. With this setting, the demapper EXIT function achieves better matching with even weaker codes such as small memory length convolution codes, and of the most practical importance is the fact that hardware complexity of the modulator and demodulator remains the same as that with the original 2^m-QAM.

In this paper, we propose for the demapper-decoder matching even simpler techniques than the combination of EM and short memory convolution coding. We first propose the EM technique combined with an extremely simple code, repetition code. It is shown that even with this very simple combination, the EXIT curves of the demapper and decoder match well, and we can achieve the BER pinch-off at relatively low SNR. However, if we combine the EM and repetition coding techniques alone, the adjustable parameters in this case is very limited, which are allocated bits (l_{map}) per symbol for EM and repetition times only. This paper then presents a factor graph representation of the system described above where it is shown that the repetition code decoder corresponds to the variable node decoder of LDPC decoder. Then, we introduce check nodes to the structure described above, which further pushes the EXIT curve of the decoder to the right side, resulting in lower BER floor. Furthermore, we also introduce irregular degree allocations to the variable node, with the aim of attaining more flexibility in changing the EXIT curve shape. It should be noticed that iterations only between the demapper

This work was supported by the Japanese government funding program, Grant-in-Aid for Scientific Research (B), No. 20360168.

and variable node decoder are required with the proposed techniques, and no iterations are needed in the decoder itself.

The paper is organized as follows. The system model is described in Section II. The basic structure of the proposed technique comprised of only EM and repetition code is introduced in Section II (A), and the improved structure comprised of variable and check nodes with regular degree distribution in Section II (B). EM BICM-ID with irregular node allocation is presented in Section II (C). The notations, (A), (B), and (C), are commonly used in this paper to identify the structures. Their convergence performances are evaluated in Section III using EXIT chart, and chain simulation results are shown in Section IV. Finally Section V concludes this paper.

II. System Model

A schematic diagram of the proposed BICM-ID system is shown in Fig. 1.

Transmitter

The binary bit information sequence $\underline{u}$ to be transmitted is encoded by (A) a simple repetition code, (B) a single parity check code where a single parity bit is added to every d_c-*1* information bits, followed by a repetition code. d_c is referred to as check node degree. The structure (C) is the same as (B), but the repetition times d_v, referred to as variable node degree, take different values in one whole block (transmission frame); if d_v takes several different values in a block, such code is referred to as having irregular degree allocation. It is assumed that throughout the paper d_c takes only one identical value as in [4].

The coded bit sequence, encoded by the encoder (A), (B), or (C), is first bit-interleaved, segmented into l_{map}–bit segments, and then the each segment is mapped on to one of the 2^m constellation points for modulation. Since $l_{map}>m$ with the EM technique, more than one labels having different bit patterns in the segment are mapped on to each constellation point. However, there are many possible combinations of bit patterns to be allocated to the constellation points. This paper uses the labels assigned to the each constellation point, obtained by [6], so that, with full *a* priori information, the mutual information (MI) between the coded bit and the demapper output extrinsic LLR at the right most point of the demapper EXIT curve is maximized. Fig. 2 shows the optimal labeling for 4-QAM with l_{map}=3 and 5. The complex-valued signal modulated according to the mapping rule, referred to as Ψ, is finally transmitted to the wireless channel.

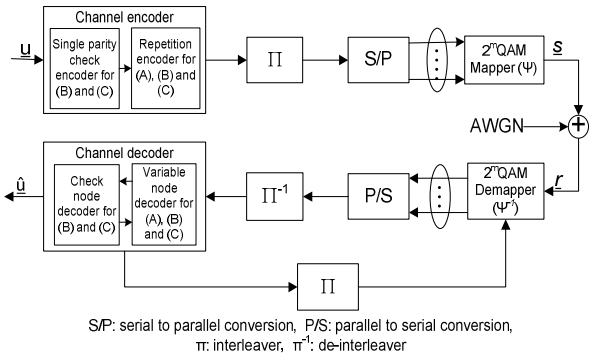

Fig. 1. System model

Channel

This paper assumes frequency flat block fading additive white Gaussian noise (AWGN) channel. If the channel exhibits frequency selectivity due to the multipath propagation, the receiver needs an equalizer to eliminate the inter-symbol interference. However, combining the technique presented in this paper with the turbo equalization framework [9]-[12] is rather straightforward.

It is assumed that transmission chain is properly normalized so that the received symbol energy-to-noise power spectral density ratio $E_s/N_0 = 1/\sigma_n^2$; with this normalization, we can properly delete the channel complex gain term from the mathematical expression of the channel. The discrete time description of the received signal $y(k)$ is then expressed by

$$y(k)=x(k)+n(k), \tag{1}$$

where, with k being the symbol timing index, $x(k)$ is the transmitted modulated signal with unit power, and $n(k)$ the zero mean complex AWGN component with variance σ_n^2 (i.e., $<|x(k)|^2>=1$, $<n(k)>=0$, and $<|n(k)|^2>=\sigma_n^2$).

Receiver

At the receiver side, the iterative processing is invoked, where extrinsic information is exchanged between the demapper and decoder. The extrinsic LLRs calculated by soft input soft output (SISO) decoding/demapping are fed back and used for demapping/decoding as *a* priori LLR; the iteration continues until no more relevant gains in extrinsic MI can be achieved [13]; when such convergence point is reached, binary decisions are made on the information bits based on the *a* posteriori LLR at the variable node. Therefore, the larger the MI at the convergence point, the lower the BER floor, which is depending on the matching between the encoder and the mapping rule.

The demapper calculates from the received signal point $y(k)$, corrupted by AWGN, the extrinsic LLR of the μ^{th} bit in the symbol transmitted at the k^{th} symbol timing, by

$$L_e[b_\mu(k)] = \ln \frac{\sum_{s\in S_0} \exp\left\{-\frac{|y-s|^2}{\sigma_N^2}\right\} \prod_{v=1,v\neq\mu}^{l_{map}} \exp(-b_v(s)L_a(b_v(s)))}{\sum_{s\in S_1} \exp\left\{-\frac{|y-s|^2}{\sigma_N^2}\right\} \prod_{v=1,v\neq\mu}^{l_{map}} \exp(-b_v(s)L_a(b_v(s)))}. \tag{2}$$

where s denotes a signal point in the constellation, $S_0(S_1)$ indicates the set of the labels having the μ^{th} bit being *0*(*1*), and $L_a(b_v(s))$ the *a* priori LLR fed back from the decoder

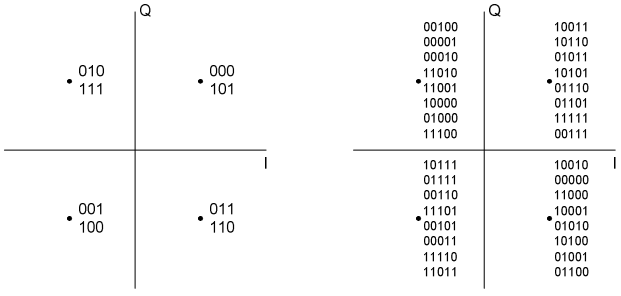

Fig. 2. Extended mapping 4-QAM l_{map}=*3* and l_{map}=*5*, optimized with *a* priori information

corresponding to the v^{th} position in the label allocated to the signal point s.

A. Repetition Coded EM BICM-ID

Fig. 3 (A) shows a block diagram of the decoder with the structure (A). The d_v bits constituting one segment, output from the de-interleaver, are connected to one variable node, where the a priori LLR to be updated is calculated by summing up the (d_v-*1*) LLRs, as

$$L_{e,j} = \sum_{i=1, i\neq j}^{d_v} L_{a,i} \quad , \tag{3}$$

to produce the extrinsic LLR for the j^{th} bit in the segment. This process is performed for all the other bits in the same segment as well as for all the other segments independently in the frame. Finally, the updated extrinsic LLRs are interleaved, and fed back to the demapper. With the *a* priori LLRs provided in the form of the decoder's output extrinsic LLR, demapper again performs the processing of Eq. (2) to update the demapper output extrinsic LLRs. This process is repeated. Obviously, the rate of this code is *1/dv*, and the spectrum efficiency is l_{map}/d_v bits per symbol.

B. Repetition Coded EM BICM-ID with Check Nodes

Fig. 3 (B) shows a block diagram of the decoder with the structure (B). The d_v bits constituting one segment, output from the de-interleaver, are connected to a variable node, and d_c variable nodes are further segmented and connected to a check node decoder; those demapper output bits in one segment, connected to the same variable node decoder, are not overlapping with other segments, and so is the case of the variable node segmentation. Therefore, no iterations in the decoder are required. The extrinsic LLR update for a bit at the check node is exactly the same as the check node operation in the LDPC codes, as

$$L_{e,cnd,k} = \sum_{i=1, i\neq k}^{d_c} \boxplus L_{a,cnd,i} \quad , \tag{4}$$

where $\sum\boxplus$ indicates the box-sum operator [14].

The extrinsic LLR, calculated by the check node decoder, is fed back to its connected variable node decoder, where it is further combined with (d_v-*1*) apriori LLRs forwarded from the demapper via the de-interleaver, as

$$L_{e,j} = L_{e,cnd,k} + \sum_{i=1, i\neq j}^{d_v} L_{a,i} \quad . \tag{5}$$

This process is performed for the other bits in the same segment, and also for all the other segments independently in the same transmission block. Finally, the updated extrinsic LLRs obtained at the each variable node are interleaved, and fed back to the demapper. With the *a* priori LLRs provided in the form of decoder's output extrinsic LLR, demapper again performs the processing of (2) to update the demapper output extrinsic LLRs. This process is repeated. The rate of this code is $(d_c - 1)/(d_c \cdot d_v)$, and the spectrum efficiency is $l_{map} \cdot (d_c - 1)/(d_c \cdot d_v)$ bits per symbol.

C. Irregular Degree Allocations

Fig. 3 (C) shows a block diagram of the decoder with the structure (C). The segment-wise structure of (C) is exactly the same as that of (B), but the variable node degrees $d_{v,i}$ may have different values segment-by-segment. The equations for the LLR update are also the same as that for (B), but the calculations have to reflect different values $d_{v,i}$ of the variable node degrees. The rate of the code is $(d_c\text{-}1)/(d_c \cdot \sum a_i \cdot d_{v,i})$, and the spectrum efficiency is $l_{map} \cdot (d_c\text{-}1)/(d_c \cdot \sum a_i \cdot d_{v,i})$ bits per symbol, where a_i represents the ratio of variable nodes having degree $d_{v,i}$ in a block.

III. Design Based on EXIT Chart

Fig. 4 shows EXIT curves for 4-QAM demappers with l_{map} as a parameter, where the labels were determined so that the EXIT curve has the largest decay. Also, the EXIT curve with Gray mapping is presented in the figure. It is found that the Gray mapping has a completely flat EXIT curve, while anti-

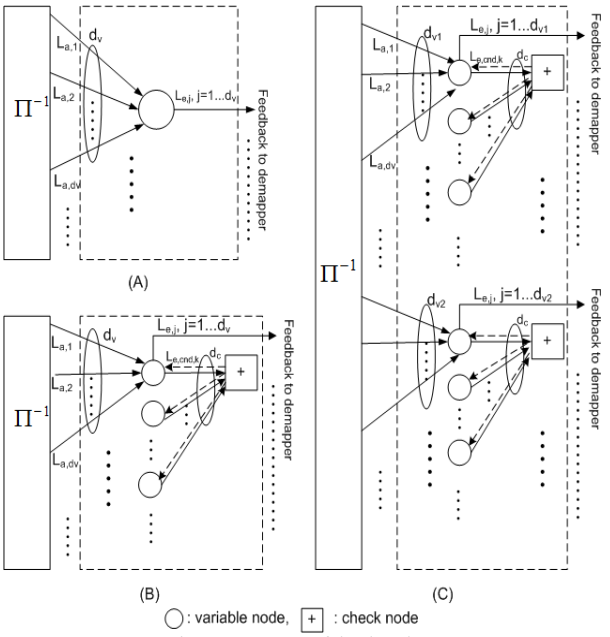

Fig. 3. Structures of the decoders

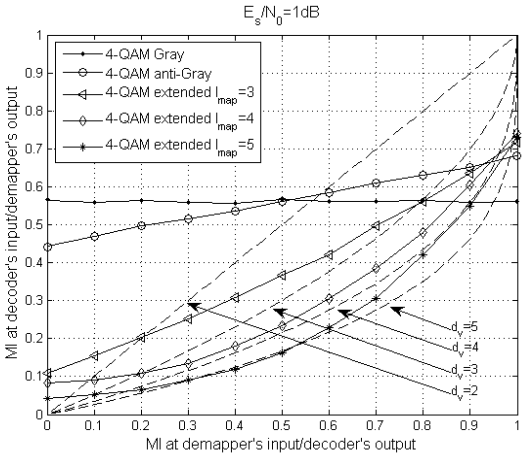

Fig. 4. EXIT chart: 4-QAM extended mapping l_{map}=*2,…,5* combined with repetition code d_v=*2,…,5*

Gray mapping has a decay. With $l_{map}=m$, since mapping rule does not change the constellation constraint capacity (CCC), the area under the EXIT curves has to stay almost the same so far as the same modulation is used ($m=constant$). With EM, the left most point is further decreased, and the right most point increased. However, the area under the curve is smaller than without EM, because even with $l_{map}>m$, still the spectrum efficiency of the modulation itself stays the same (m).

A. Repetition Code

With the Gaussian assumption for the LLR distribution, the EXIT function of the repetition code is given by

$$I_{e,v} = J\left(\sqrt{(d_v - 1)\cdot J^{-1}\left(I_{a,v}\right)^2}\right). \quad (6)$$

where $I_{a,v}$ is the variable node input *a* priori MI and $I_{e,v}$ is its output extrinsic MI. $J()$ and $J^{-1}()$ are the functions that convert the square-root variance σ of LLR to its corresponding MI, and its inverse, respectively [2]. Obviously, (6) is corresponding to (3) for LLR update, with which $I_{a,v}= I_{e,dem}$ with $I_{e,\,dem}$ being the demapper output extrinsic MI.

B. Repetition Code with Check Node

The check node EXIT function can be approximated by [15]

$$I_{e,cnd} = 1 - J\left(\sqrt{d_c - 1}\cdot J^{-1}\left(1 - I_{a,cnd}\right)\right), \quad (7)$$

where

$$I_{a,cnd} = J\left(\sqrt{d_v \cdot J^{-1}\left(I_{a,dec}\right)^2}\right). \quad (8)$$

The EXIT function of the whole decoder comprised of the variable and check node decoders can be calculated by combining Eq. (6) and (7) [4], as

$$I_{e,dec} = J\left(\sqrt{(d_v - 1)\cdot J^{-1}\left(I_{a,dec}\right)^2 + J^{-1}\left(I_{e,cnd}\right)^2}\right), \quad (9)$$

with $I_{a,dec}= I_{e,dem}$.

C. Irregular Repetition Code with Check Node

The EXIT function of the whole decoder with the structure (C) can be obtained by weighting the segment-wise EXIT functions given by (9), by a_i corresponding to their distributions, as

$$I_{e,dec} = \frac{\sum_i a_i \cdot d_{v,i} \cdot J\left(\sqrt{(d_{v,i} - 1)\cdot J^{-1}\left(I_{a,dec}\right)^2 + J^{-1}\left(I_{e,cnd}\right)^2}\right)}{\sum_i a_i \cdot d_{v,i}}. \quad (10)$$

Hence, the shape of the combined code EXIT function can be flexibly controlled so that better matching between demapper and decoder curves can be achieved.

Fig. 5 shows EXIT functions of the decoders (A), (B), and (C) for the degree allocations presented in the box in the figure, where the code rates are *1*, *0.99*, and *1.29*, respectively. It is found by comparing Figs. 4 and 5 that the EXIT functions of EM and the repetition code with check nodes can be well matched by changing the degree allocations a_i, by which we can expect sharp turbo cliff to happen at their corresponding threshold E_s/N_0, even though the structures of (A), (B), and (C) are very simple and easy to implement.

IV. Numerical Results

A series of simulations was conducted with enough number of bits transmitted to verify the advantageous characteristics of the techniques proposed. As described above, the EM technique does not change the CCC, and therefore the capability of achieving near capacity performance even with the very simple structure, which is the most significant advantage of the proposed technique, is mostly in a low E_s/N_0 value range (or equivalently low rate code case). If the CCC is much lower than the Gaussian capacity at the system's operation E_s/N_0 point, no significant merit can be expected, and obviously larger modulation format should be used in such case.

In Fig. 6, we compare BERs of EM 4-QAM with 32-QAM M32a mapping [16], both by using repetition code with structure (A), while keeping the system spectrum efficiency at *1* bit-per-symbol. It is found from the figure that, the BER of $l_{map}=3$ EM 4-QAM with $d_v=3$ repetition code only slowly decreases as E_s/N_0 increases, while, with $l_{map}=5$ EM 4-QAM with $d_v=5$ repetition code, the turbo cliff happens at $E_s/N_0=1.4dB$. Fig.7 shows for $E_s/N_0=1.4dB$ the EXIT functions of the demapper and the decoder for $l_{map}=5$ and $d_v=5$. Also, the MI trajectory obtained as a result of the chain simulation is shown in the figure. It is found from the figure that the EXIT curves and the trajectory exactly match with each other. Furthermore, with $E_s/N_0=1.4dB$, the tunnel is open until the point where the decoder output extrinsic $MI=0.994$, which

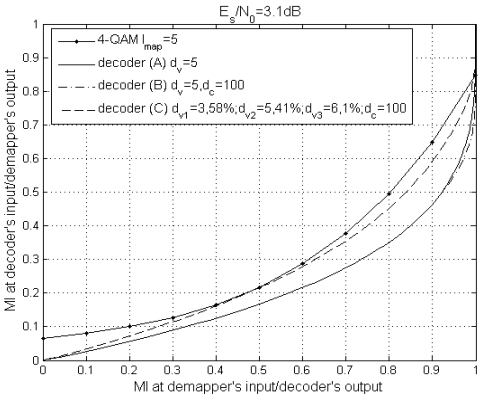

Fig. 5. EXIT chart: 4-QAM EM lmap=5 combined with 3 kinds of repetition code due to structures (A), (B) and (C)

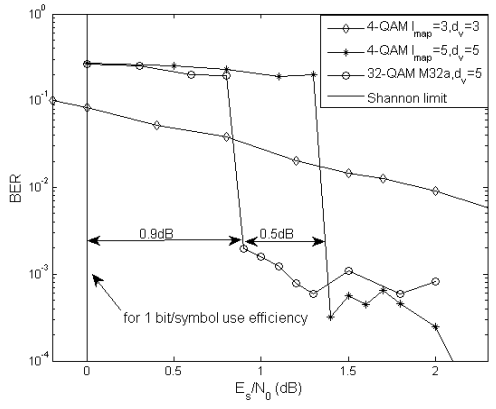

Fig. 6. BER curves of 3 different mappings combined with repetition code

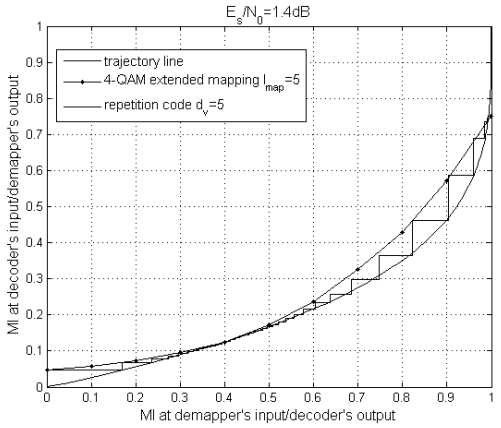

Fig. 7. EXIT chart: 4-QAM EM $l_{map}=5$ combined with repetition code $d_v=5$

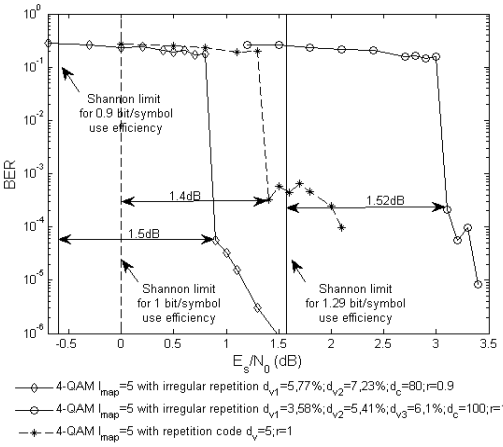

Fig. 8. BER curves optimized by irregular repetition code

corresponds to the a posteriori *MI=0.998,* yielding the error floor of 3.4×10^{-4}. Those observations are exactly consistent to the BER curve shown in Fig. 6. It is also found from Fig. 6 that with 32QAM M32a mapping, a turbo cliff happens at $E_s/N_0=0.9dB$, which is *0.5dB* closer to the Shannon limit for 1 bit-per-symbol spectrum efficiency than with $l_{map}=5$ EM 4-QAM and $d_v=5$ repetition code. This is because the EXIT function of 32QAM M32a mapping better matches with that of the $d_v=5$ repetition code decoder. However, it should be emphasized here that modulation and demodulation hardware for the $l_{map}=5$ EM 4-QAM is exactly the same as that for simple 4-QAM, while that for 32QAM is much more complex. Therefore, the 0.5dB loss in E_s/N_0 at the turbo-cliff point can well be compensated by the hardware complexity reduction.

With the structure (A), the adjustable parameters are only l_{map} and d_v. We therefore introduce the check node in (B), and furthermore, irregular degree allocation in (C), both to (A). Two BER curves with $l_{map}=5$ EM 4-QAM with structure (C) are shown in Fig. 8, together with that, with $l_{map}=5$ EM 4-QAM and $d_v=5$, to demonstrate the design flexibility. The degree allocations are shown under the figure caption. In fact, the allocation parameters for the rate *1.29* code, of which BER is indicated by "o" in the figure, are exactly the same as that shown in Fig. 5 for (C) with $E_s/N_0=3.1dB$. It is found that the EXIT and BER curves, presented in Figs. 5 and 8, are exactly consistent with each other (at $E_s/N_0=3.1dB$, EXIT tunnel opens and BER turbo cliff happens). These observations indicate that with the design flexibility made available by introducing the irregular structure, we can flexibly control the threshold E_s/N_0 and the error floor.

V. CONCLUSIONS

In this paper, we have proposed a combined use of extended mapping (EM) and repetition coding. It has been shown that even with this extremely simple structure, we can achieve excellent matching between the demapper and decoder EXIT curves. Furthermore, we have introduced check node as well as irregular degree allocation on to the structure described above. With the design flexibility made available by introducing the check node and irregular structure, we can flexibly control the shape of the decoder EXIT function to achieve better matching between the two curves. It has also been shown that BER curves obtained through chain simulations are exactly consistent to the EXIT analysis result for the structures proposed in this paper. Finally, it should be emphasized that the complexity for the proposed technique is extremely low, because EM does not require higher order modulation format and no iterations are needed in the decoder itself.

REFERENCES

[1] G.Caire, G.Taricco and E.Biglieri, "Bit-Interleaved Coded Modulation", IEEE Trans. on Inform. Theory, vol.44, no.3, pp. 927-946, May 1998.

[2] S. ten Brink, "Convergence Behavior of Iteratively Decoded Parallel Concatenated Codes", IEEE Trans. on Comm., vol.49, pp. 1727–1737, Oct. 2001.

[3] J. Hagenauer, "The EXIT Chart - introduction to extrinsic information transfer in iterative processing", 12th European Signal Processing Conference (EUSIPCO), pp. 1541–1548, 2004.

[4] S.ten Brink, G.Kramer, A.Ashikmin, "Design of low-density parity-check codes for modulation and detection", IEEE Trans. on Comm., vol.52, pp. 670-678, June 2004.

[5] F. Schreckenbach, N. Görtz, J. Hagenauer, G. Bauch. "Optimized Symbol Mappings for Bit-Interleaved Coded Modulation with iterative decoding", IEEE GLOBECOM'03, vol.6, pp. 3316-3320, Dec. 2003

[6] T. Clevorn and P. Vary, "Iterative Decoding of BICM with Non-Regular Signal Constellation Sets", International ITG Conference on Source and Channel Coding, 2004.

[7] P. Henkel, "Extended Mappings for Bit-Interleaved Coded Modulation", IEEE PIMRC, pp. 1-4, 2006.

[8] P. Henkel, "Doping of Extended Mapping for Signal Shaping" In Vehicular Technology Conference, 2007. VTC2007-Spring, IEEE 65th.

[9] M. Tuchler, R. Koetter, and A. Singer, "Turbo equalization: principles and new results", IEEE Trans. Comm., vol. 50, pp. 754-767, 2002a.

[10] X. Wang and H.V. Poor, "Iterative (turbo) soft interference cancellation and decoding for coded CDMA", IEEE trans. on Comm., vol. 47, pp. 1046-1061, 1999.

[11] T. Abe and T. Matsumoto, "Space-time turbo equalization in frequency-selective MIMO channels", IEEE Trans. Veh. Tech., vol.52, pp. 469-475, 2003.

[12] L. Hanzo, T.H. Liew, and B.L. Yeap, "Turbo Coding, Turbo Equalization and Space-Time Coding for Transmission over Fading Channels", Wiley-IEEE Press, 2002.

[13] S. ten Brink, "Convergence of iterative decoding", Electronics Letters, vol.35, pp.806–808, May 1999.

[14] J. Hagenauer, E. Offer, L. Papke, "Iterative decoding of binary block and convolutional codes", IEEE Trans. on Inform. Theory, vol. 42, pp. 429-445, Mar. 1996

[15] Shu L., Daniel J., Costello Jr., "Error Control Coding (2nd Edition)", Prentice Hall, June 2004.

[16] F. Schreckenbach and G. Bauch, "Bit-interleaved coded irregular modulation", European Transactions on Telecommunications, vol.17, pp. 269–282, March/April 2006.